inter.noise
27-30 AUGUST HONG KONG 2017

Noise radiation from steel bridge structure – Old Årsta bridge Stockholm

Anders Olsen[1]; René Smidt Lützen[2]; Stewart Holmes[3]

[1] Vibratec Akustikprodukter ApS, Denmark

[2,3]Lloyd's Register, Denmark

ABSTRACT

The 1929 Old Årsta bridge in central Stockholm (Sweden), owned and operated by the Swedish Transport Administration(Trafikverket), is a monumental structure of architectural value and infrastructural importance to the city. Following recent renovation work, an increase of train noise was observed. Hence, the Swedish Transport Administration decided to mitigate the noise. A multi-step project was defined to this end. The present paper presents the findings of the pre-study, the purpose of which was to investigate the noise radiation from the bridge. This involved vibro-acoustic modelling by Statistical Energy Analysis (SEA), laboratory testing of various Constrained Layer Damping (CLD) configurations at different temperatures, as well as similar CLD tests on a mock-up, noise and vibration measurements on the actual bridge, and acoustical beamforming measurements.
Keywords: Railway, Damping, Noise control I-INCE Classification of Subjects Number(s): 38

1. INTRODUCTION

Constructed in 1920 to 1929, the Old Årsta bridge is a monumental double track steel arch bridge with a steel deck and a main span of 151 m. It is located on one of the main railway lines of Stockholm (Sweden) and recently underwent refurbishment to upgrade bridge bearing capacity. This included a new bridge deck in terms of a full steel deck with welded longitudinal and transversal girders. The deck is connected to the supporting arch using hangers and columns. The track of the retrofitted deck is now based on a Pandrol VIPA rail fastening system.

Following construction of the new bridge deck, increased noise from train passages was reported. The Swedish Transport Administration initiated a project with focus on noise reduction from the bridge, including the present pre-study. Given an around the clock average interval of only 6 minutes between trains, a non-intrusive execution was required. Hence, for the investigation no access was allowed to the top of the bridge deck. Similarly, any recommended mitigation means would have to be installed from below.

To the west of Old Årsta bridge, in parallel at approximately 45 m distance, runs a newer bridge, which proved to be a useful platform for measuring train passage noise. Furthermore, to the North a concrete bridge, having the original fasteners on ballasted track as the new bridge before retrofitting, is located on the same line as Old Årsta.

2. Method

Past noise control actions for Old Årsta bridge involved modifying the track from wooden sleepers to resilient rails fasteners (2,1). Given the current restrictions on access, track modification was no longer a relevant option. Instead, focus was placed on the potential of targeting the bridge steel structure itself. Thompson (2) lists several such examples, with varying results in terms of noise reduction. In the discussion, it is mentioned that the achieved reduction was limited in general by the amount of damping already present in the untreated structure. Furthermore, the balance between rolling noise and noise radiated by the bridge structure plays a limiting role.

In certain cases, structural damping may be added using vibration absorbers (4). This solution is,

[1] ao@vibratec.dk
[2] rene.smidtluetzen@lr.org
[3] stewart.holmes@lr.org

however, quoted as being suitable only for frequencies below 150 Hz.

In this study, which was undertaken on behalf of the main contractor Skanska by Vibratec and the consulting branch of Lloyd's Register (LR), the potential of Constrained Layer Damping (CLD) for noise reduction was investigated. A general challenge of CLD solutions is the inherent temperature dependence of the viscoelastic material. However, previous successful experience was found for an outdoor industrial application in mid-continent climate (3). This was achieved using CLD patches with two viscoelastic materials, having different properties.

For Old Årsta Bridge an engineering approach was decided. An empirical investigation of noise and vibration of the existing, untreated bridge was combined with numerical simulations using SEA as well as laboratory measurements. The study outline was:

- Empirical investigation of noise, and corresponding vibration
- Identification of noise contributors, particularly train (rolling noise) vs. bridge contribution
- Establishment of prediction model
- Use of prediction model with CLD damping input from lab tests and SEA model
- Identification of the optimum CLD configuration and expected noise reduction

In the following, comments are given to the various measurements and modelling actions. The measurements were taken 5-7 April 2017 during wind speed 2-4 m/s mostly western wind and about 10°C.

2.1 Noise and vibration measurements on Old Årsta bridge and western bridge

As the study focuses on Old Årsta steel bridge, it was necessary to find a means of identifying start and stop times for trains crossing the bridge. To that end, a "train detector" system was installed. This consisted of a 1 mV/(m/s^2) accelerometer on the underside of the deck, at each end of the bridge. The individual passage of every bogie, sometimes even every wheelset, was clearly distinguishable from the recorded time series. The train detector system furthermore enabled determination of the train speed. Of the considered passages, an average of 88 km/h was found, typically ranging from 80 to 95 km/h.

Using a multi-channel, 24 bit data acquisition system, the train detector accelerometers were recorded to a laptop in parallel with 5 accelerometers of sensitivity 1 mV/(m/s^2). Train passages were measured for accelerometer positions representing the main components of the bridge, collecting several passages per measurement position. Sample frequency was 6400 Hz.

Simultaneously, a separate measurement system for recording noise was placed opposite the steel bridge, at Pos A in Figure 1. This autonomous system was a sound level meter BK2270 with its microphone fitted in an outdoor microphone kit. The system continuously recorded time series with maximum useable frequency 3300 Hz, in 24 bit quality.

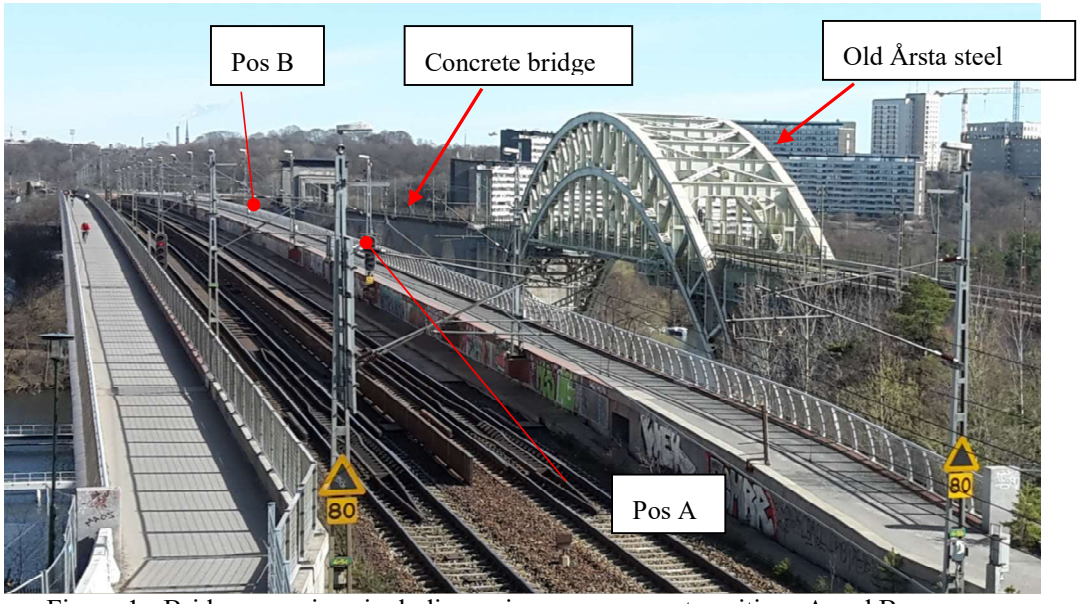

Figure 1 - Bridge overview, including noise measurement positions A and B

2.2 Microphone array measurements

At Pos B, a limited number of measurements were taken with LR's in-house developed 2D array consisting of 56 microphones, see Figure 2. A sample rate of 5000 Hz was used. These were taken at the end of the measurement campaign, when the train detector system had been disabled, hence, train speeds were unknown.

Figure 2 – Microphone array in front of steel bridge, Pos A.

The spatial resolution from the applied position was insufficient for directly separating noise contributions from train, rails, and bridge using basic Delay and Sum algorithm. However, a few useful observations were indeed made. The array included a centred and calibrated camera, providing one still image per train passage.

2.3 Structural dynamic measurements

2.3.1 Point mobility of bridge components

Point mobility was measured of several components of the Old Årsta bridge, using an instrumented impact hammer of 0.26 mV/N and a magnet mounted accelerometer of sensitivity 100 mV/(m/s^2). An LR in-house tool was used for processing complex FRF spectra as an average of 5-10 hits per position, with no data window applied. These were input to industry standard modal analysis software BK PULSE Reflex Modal. The Rational Fraction Polynomial-Z algorithm was applied to extract natural frequencies and damping ratio for each measurement position, for the frequency range 50-1000 Hz.

2.3.2 Lab test of temperature dependent CLD damping

At LR's lab a climatic chamber was established to test the structural damping of an 18 mm x 70 mm x 1400 mm steel beam sample with several different CLD add-on treatments, designed and provided by Vibratec. The beam thickness corresponds to the deck and main girders of the Old Årsta bridge components. The width and length were selected to ensure bending modes starting at 50 Hz, to represent the bridge plating as well as possible. At temperatures, +20, +5, and -10°C the resiliently suspended beam was excited by continuous white noise from a shaker with introduced force transducer. The vibration response was captured with 7 accelerometers. Post-processed FRF spectra were, as in Section 2.3.1, introduced to modal analysis software and analysed up to 1000 Hz. Analysis was performed with combinations of Rational Fraction Polynomial-Z, Alias-Free Polyreference, and Polyreference Time, depending on the properties of the test specimen. Mode shapes were used qualitatively to separate bending modes from torsion and lateral modes, as only bending modes were considered relevant for the noise control of Old Årsta bridge. This approach provided temperature and frequency damping ratio estimates, which should be regarded as engineering linear approximations of the non-linear viscoelastic behaviour.

2.3.3 Large-plate mock-up test with different CLD configurations

At Vibratec's workshop in Estonia, an indoor test at approximately 15°C was performed on a 18 mm x 1400 mm x 2000 mm steel plate elastically suspended from a crane. For 6 different CLD configurations, random impacting was performed with a hammer, and the vibration was recorded with two accelerometers. The resulting vibration time series were input to industry standard Operational Modal Analysis software ARTeMIS Modal and analysed using Stochastic Subspace Identification (SI) algorithms as well as Enhanced Frequency Domain Decomposition (EFDD).

2.3.4 Numerical Statistical Energy Analysis model for insertion loss

Commercial software VAOne for Statistical Energy Analysis (SEA) was used for establishing a numerical, vibro-acoustic model of the bridge without hangers and arches, see Figure 3.

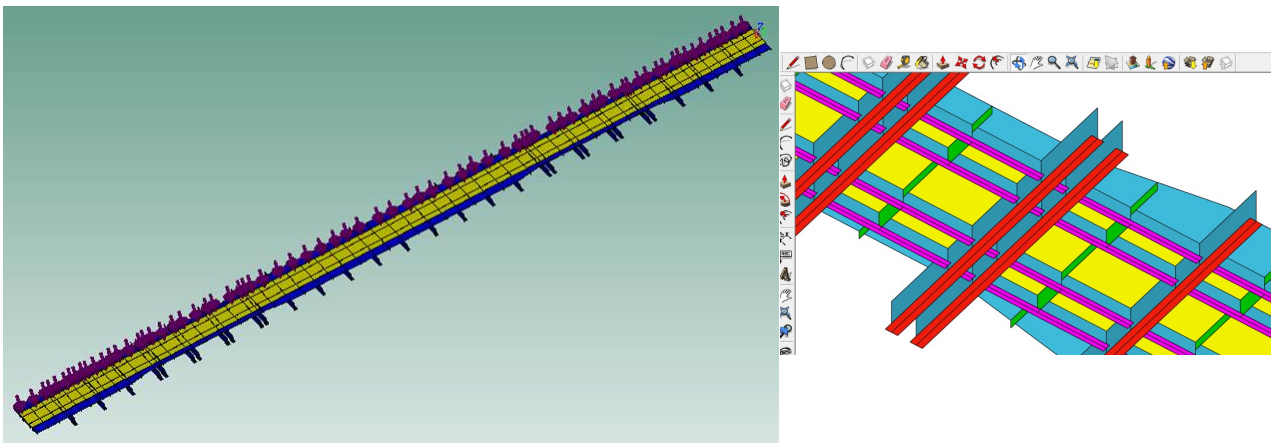

Figure 3 – SEA model of bridge. Left: from above. Right: Detail from below (arches not modelled)

In the left image of Figure 3 the little purple arrows indicate a line of distributed, vertical uncorrelated point forces placed in the centre line of one track. They were assigned white noise with 1 N amplitude each. With this excitation, the SEA model was used to calculate the un-calibrated resulting noise in a horizontal distance of 45 m, corresponding to the physical Pos A of Figure 1. This was first done with low-level structural damping assigned to all bridge elements, corresponding to the present stage of the untreated bridge. Subsequently, CLD configurations were investigated by assigning the lab test damping of Section 2.3.2 to individual bridge components, and calculating the un-calibrated resulting noise. Subtraction from the noise of the untreated bridge thus provided an insertion loss corresponding to that particular CLD configuration. The SEA model output was presented in 1/3-octave bands from 160 to 2500 Hz.

2.3.5 Combined prediction model

A simple prediction model was established, describing the noise contribution at Pos A for each major bridge component (deck, longitudinal girders, flanges of longitudinal girders, etc.). The model combined statistically averaged vibration spectra with radiation index spectra. The resulting sound power spectra were propagated to the distance of Pos A using a simple spherical spreading law.

For prediction of the various CLD configurations, the measured input vibration spectra of the untreated bridge were first corrected for insertion losses. The latter were either calculated using the SEA model of Section 2.3.4, or using simple algebraic expressions proportional to the relative increase of damping ratio.

2.4 Considered CLD configurations

10 different CLD configurations were tested in the climate chamber at LR. The CLD's varied from either simple single layers to multi-layer solutions. Previous experience (3) with CLD configurations in temperature dependent applications indicated that single layers only provide high performance in either high or low temperature environment, depending on the properties of the damping material.

Therefore, the relevance of combining damping materials is essential and reported in the literature, for example (5).

In this project, two different damping materials were used. Each material consisted of a 1.4 mm bitumen layer, with viscoelastic glue on each side with release liner. Only difference between the two types is the viscoelastic glue.

The damping materials are usually manufactured in sheets of 1000 mm x 1000 mm with release paper on each side, for easy mounting.

The two basic damping material solutions used in this project are shown in Figure.4.

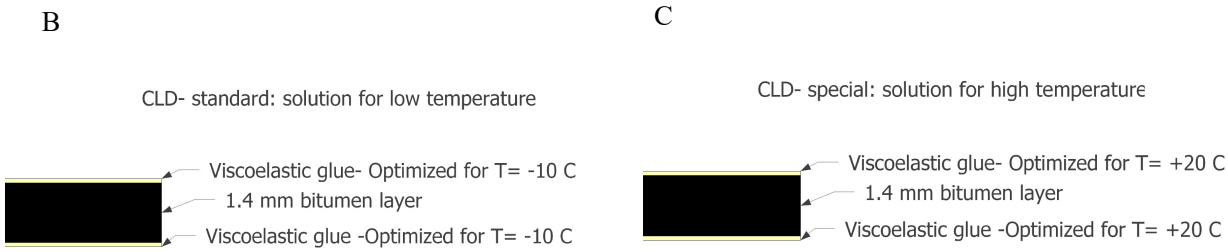

Figure 4- Damping material compositions. B for CLD-standard & C for CLD-special

Each type of material is normally considered as a single layer, however note that this is a 3-layer system, since glue as well as bitumen layer has viscoelastic behavior.

These two materials were used in the 10 CLD configurations that are shown in Figure 5.

The following terms are used for simplicity:
A: Steel beam sample (18 mm thick)
B: CLD-Standard (app. 2 mm including glue)
C: CLD-Special (app. 2 mm including glue)
D: Sandwich steel bar (2 mm)
E: Sandwich steel bar (1 mm)
F: Constraining steel bar (3 mm)
G: Constraining steel bar (5 mm)

Sample ID	**Layer configuration**	**Type of CLD composition**	**Total thickness of CLD patch**
1	**A**/B/**G**	Single layer(winter)	7 mm
2	**A**/C/**G**	Single layer(summer)	7 mm
3(shaker ref. A)	**A**/(B/C)/**G**	Single layer. 50 % of sample with CLD special and 50 % CLD standard	7 mm
4	**A**/(2xB/C)/**G**	Double layer of CLD. Arranged in cross pattern	9 mm
5	A/C/**D**/B/**F**	Multi-layer	9 mm
6	**A**/B/**D**/C/F	Multi-layer	9 mm
7	**A**/(2XB/C)/**G**	Double layer of CLD. 50 % of sample with CLD special and 50 % CLD standard	9 mm
8	**A**/B/C/**G**	Double layer	9 mm
9(shaker ref. I)	**A**/C/B/**G**	Double layer	9 mm
10	**A**/(B/C)/**E**/(B/C)/**G**	Multi-layer	9 mm

Figure 5- CLD configurations for test

In order to have the most realistic setup in relation to real world application, each of the CLD configurations were mounted on the 18 mm steel beam, using weld studs. This ensured that local de-bonding was minimized. A torque of 30-50 Nm was used for tightening of the lock bolts, depending

on the manufacturing tolerance of the steel bars. For structural and practical reasons the weight of the CLD systems are restricted to app. 40-45 kg/m^2, which mean that the max. thickness of the constraining steel plate is app 5.0 mm. Generally, for CLD systems, increased thickness of the constraining plate leads to increased damping ratio.

Local de-bonding of damping layers will have an influence on the measurements and lower the damping ratio, due to non-contact zones. However, in real applications it is very difficult to completely avoid this. Weld studs are also used in real installation, as CLD patches are mounted vertical and below steel decks, which mean that gravity forces will influence the contact pressure.

No numerical or analytical estimates were performed for the composite damping ratio of the various configurations, as the general Ross, Kerwin and Ungar (RKU) equations (5,6) are only valid for simple configurations such as sample IDs 1 and 2. Multi layers may be predicted with RKU equations, but given the limited information of the viscoelastic glue damping properties, the theoretical and analytical approach is difficult. Understanding the viscoelastic glue better will require several measurements and extraction of the damping ratio as well as complex E-modulus of the glue.

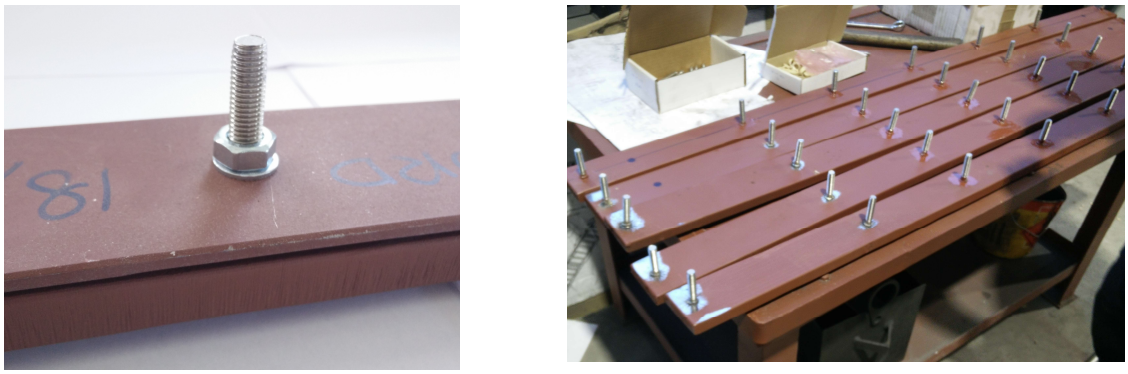

Figure 6- Left picture- final CLD sample. Right picture- Steel beam with weld studs

3. Results

3.1 Findings from noise and vibration at steel bridge

Figure 7 shows passage noise spectra at Pos A, synchronised from the train detector system to precisely the passage of the steel bridge. Due to the intense traffic on both parallel bridges care had to be exercised to identify undisturbed passages with only one train at a time. A total of 8 undisturbed passages were identified. Based on time synchronization with the train detectors, 1/3-octave band spectra corresponding to the passage of the steel bridge were extracted, see Figure 7.

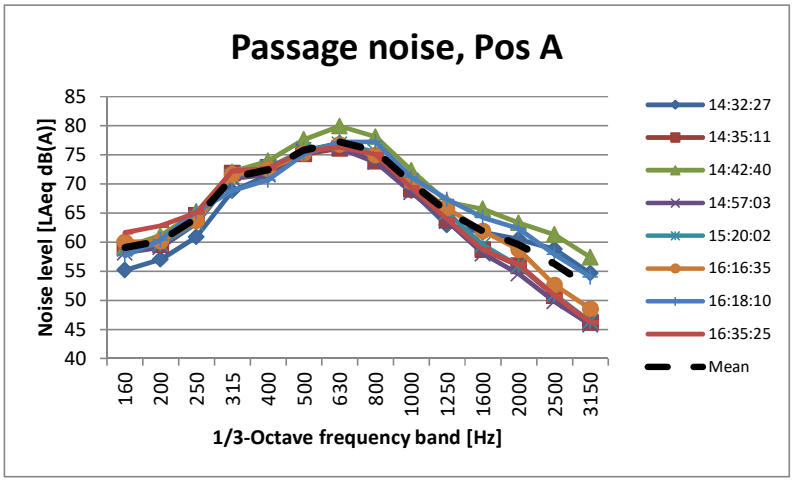

Figure 7– A-weighted 1/3-octave band spectra at Pos A (in front of steel bridge).

The passage time was typically about 6 s, and the average overall noise level was 83 dB(A), with a standard deviation of 1 dB. In Figure 7 it is seen that the noise is dominated by the 500-800 Hz range. It is seen that the range 250-800 Hz has relatively little spread, while the passages vary much more for higher frequencies. Realizing that train wheels typically become effective acoustic radiators above about 1 kHz, this might indicate that the noise contribution below 1 kHz is dominated by the bridge properties, while noise about 1 kHz is more strongly influenced by the individual vehicle.

At one point the train detectors were not in operation, a handheld sound level meter BK2250 was used to measure at Pos B in front of the concrete bridge. For the same train passing the steel bridge, the corresponding spectrum was extracted from Pos A. One such example is shown in Figure 8.

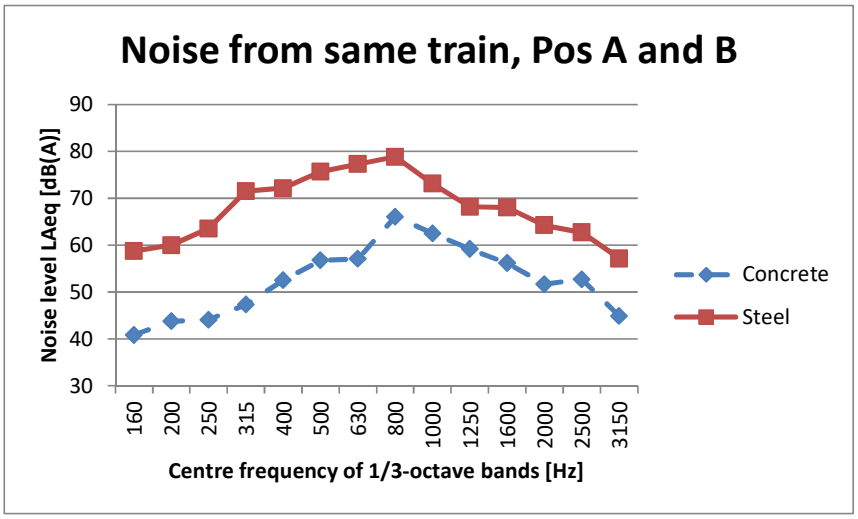

Figure 8– A-weighted 1/3-octave band spectra for same train, in front of concrete and steel bridges.

In Figure 8, the spectrum from the front of the steel bridge is clearly louder than in front of the concrete bridge. Overall levels here increased by 15 dB. Following the approach by (2) it is reasonable to assume that noise at Pos B is dominated by the train (actually, rolling noise) contribution, as the concrete bridge is unlikely to radiate significantly. Assuming that the 1-2 kHz range is dominated by the train contribution at both bridges, an increase of 10 dB in this range was determined as an average of 6 train passages. It is assumed that this is the increase in rolling noise caused by the different track and fastener types. This is in line with typical findings of 5-10 dB rolling noise increase (1). From this finding, the rolling noise on the steel bridge was predicted as the average spectrum at the concrete bridge (Pos B) plus 10 dB. The corresponding overall level was 78 dB(A).

By using the train detector system, vibration spectra of train passages were extracted for several bridge components. By means of example, the vibration spectra at deck underside positions are shown in figure 9. For the deck, an average overall level L_v of 133 dB re. 10^{-9} m/s was found, with a standard deviation of approximately 1.5 dB.

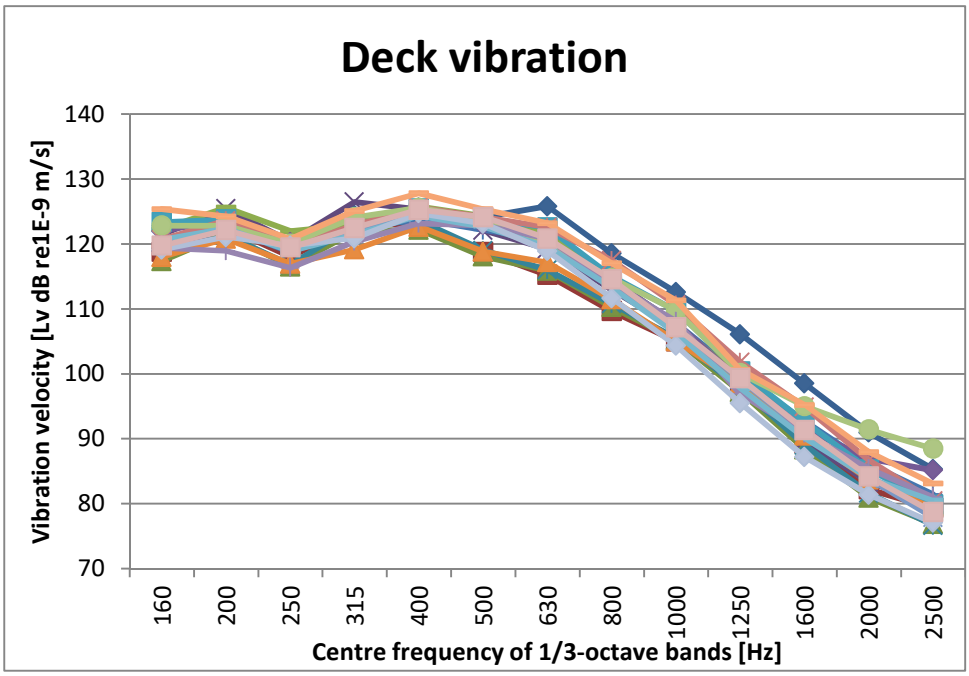

Figure 9 – Measured vibration velocity spectra of deck underside, average of 22 passages.

3.2 Findings from microphone array measurements

An array example of 1.6 s of a train passage is shown in Figure.10, for frequency range 1 to 2 kHz. The spatial resolution obtained with the array was insufficient to separate the radiating components, mainly due to the large distance between measurement position and the bridge. The colours indicate the upper 6 dB of the measured noise level range. When inspecting a sequence of analyses corresponding to the train passages (not shown here) the various "hot spots" appear fairly concentrated (as in Figure.10) and travel with the train along the bridge. It seems likely that these spots relate to the rolling noise of the bogies. It is furthermore observed that the bridge arches do not appear to radiate significantly, as they do not "light up" in these plots.

For lower frequencies, e.g. 600-800 Hz (array plot not shown), the "hot spots" became unrealistically large due to the wavelength proportional spatial resolution. Though less clear than for the kilohertz range, the "hot spots" still mostly appear round/elongated and centred in the train/deck region.

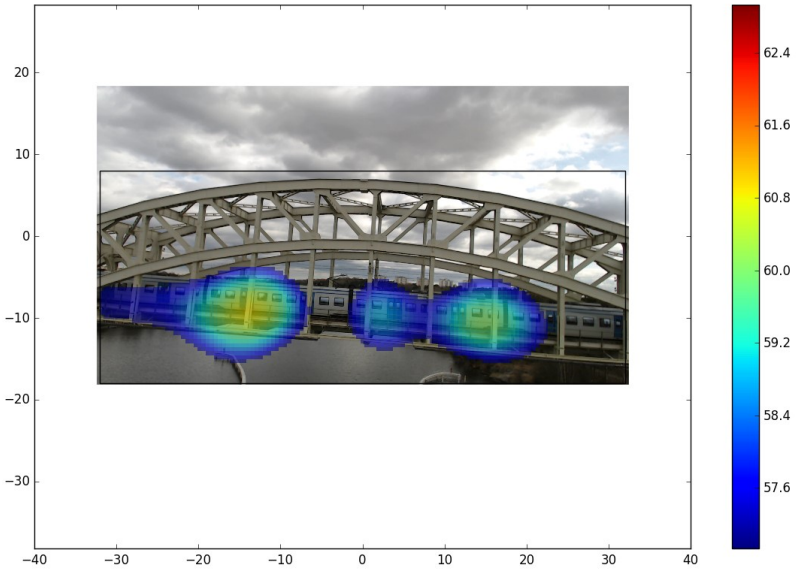

Figure. 10 – Microphone array analysis for frequency range 1-2 kHz, using Delay and Sum.

3.3 Findings from structural dynamic measurements

By means of example, Figure 11 shows a stability diagram (0-500 Hz range) of the modal analysis performed on point mobility input from a position on the longitudinal girder. Corresponding natural frequencies (0-1 kHz) and damping ratios are included. Generally, it was found for the bridge components that in the frequency range of interest the damping ratio was typically 0.5-1%. Furthermore, as in the case of the girder, lowest natural frequencies were found in the 50-100 Hz range. Both observations are positive as to the noise reduction potential of adding structural damping, as this requires many and at best low-damping, resonant modes.

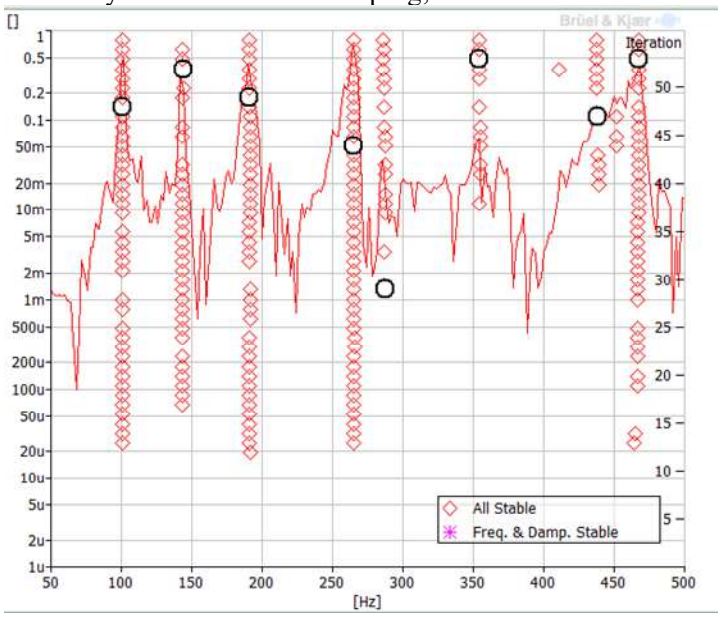

Freq [Hz]	Damp. ratio [%]
100.9	1.5
143.8	0.8
191.2	1.4
265.2	0.8
287.8	0.2
354.2	0.5
438.1	1.2
467.3	0.6
566.1	1.2
587.6	0.7
652.7	1.5
699.1	0.7
709.7	0.8
837.3	0.7

Figure 11 – Example of mobility analysis results from longitudinal girder.

From the lab climatic chamber damping tests, it was found that various CLD configurations demonstrated damping ratios up to about 14% at certain frequencies, see e.g. configuration I of Figure 1212. However, as in the case of configuration I, the same CLD performed rather poorly at other temperatures.

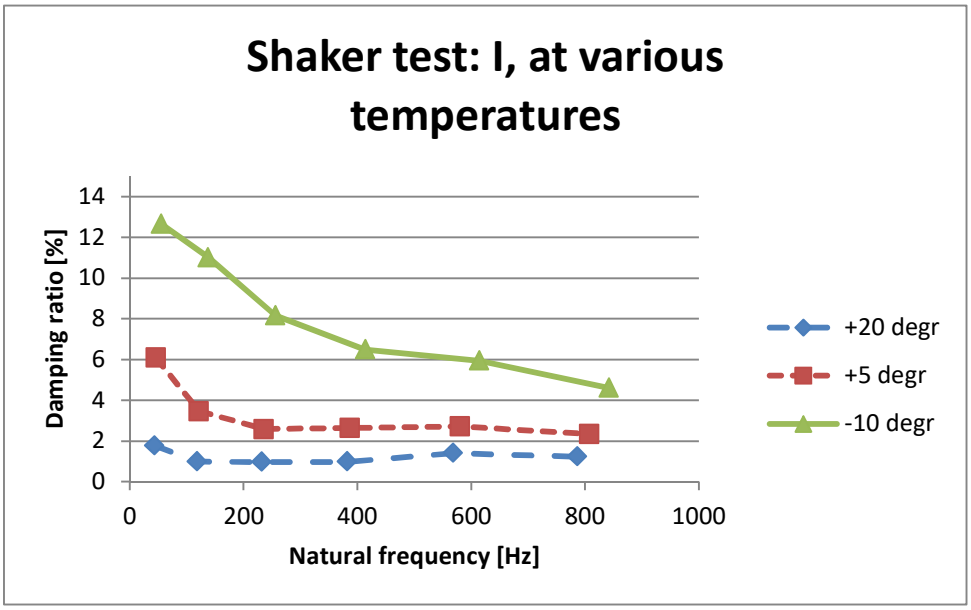

Figure 12 – Lab damping test of CLD configuration I.

Other configuration provided more consistent damping across frequency and temperature, e.g. configuration 3(Shaker ref. A) of figure 13.

The large-plate indoor test at 15°C was mostly performed on configurations derived from CLD configuration A. In the best configuration, a damping ratio of 3-4% was obtained. Comparison of 1/3, 2/3, and full surface CLD coverage showed damping ratio 1-2%, 2-2.5%, and 3-4%, respectively.

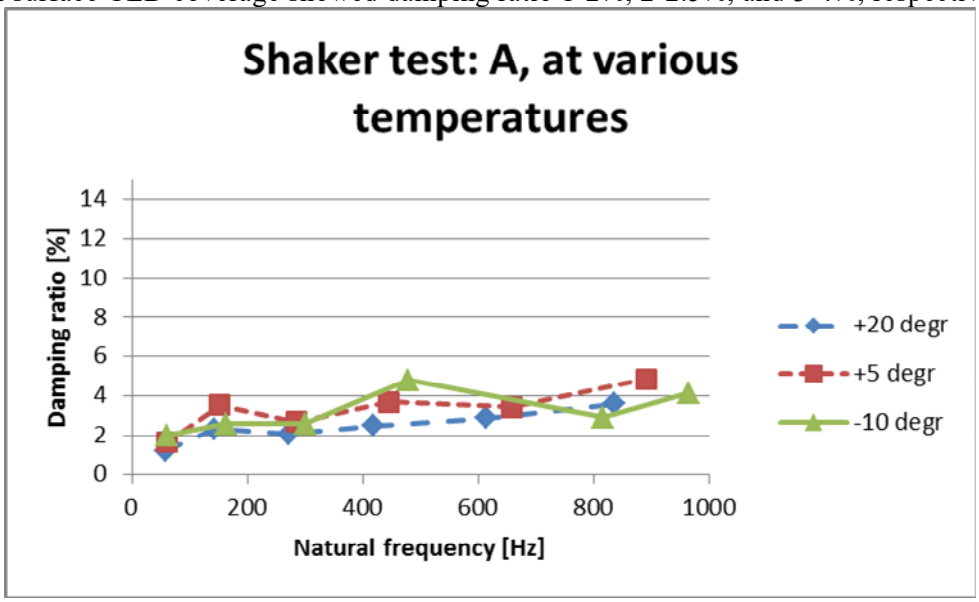

Figure 13 – Lab damping test of CLD configuration 3(shaker ref. A).

3.4 Findings from SEA model

Following a conservative approach, it was decided to assign a damping ratio of 1% to all bridge components in the untreated stage. Figure 14 illustrates that noise insertion loss IL_p of the various bridge components are generally not the same, even in the shown configuration where all plates are assigned the same damping ratio. This is a consequence of the energy- wise closely coupled set of sub-systems, with forcing taking place on one system (the deck/top plating).

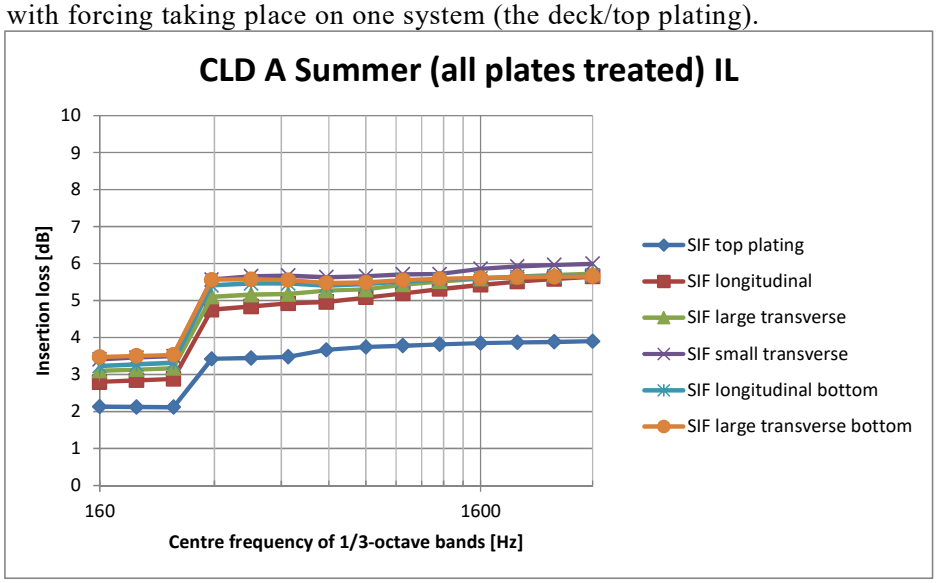

Figure 14 – Example of SEA calculated insertion loss from CLD configuration 3, summer temperature.

3.5 Findings from prediction model

In terms of overall values, the model predicted 84 dB(A), which is slightly higher than the measured 83 dB(A). Given the involved uncertainties, this seems an acceptable agreement. From figure 15 it follows that the frequency range up to 800 Hz according to the prediction model is dominated by radiated “bridge noise”, i.e. the noise produced by vibration of the bridge plating and girders. Above 800 Hz the “train”, or rolling, noise takes over and dominates. This is in line with expectations from literature.

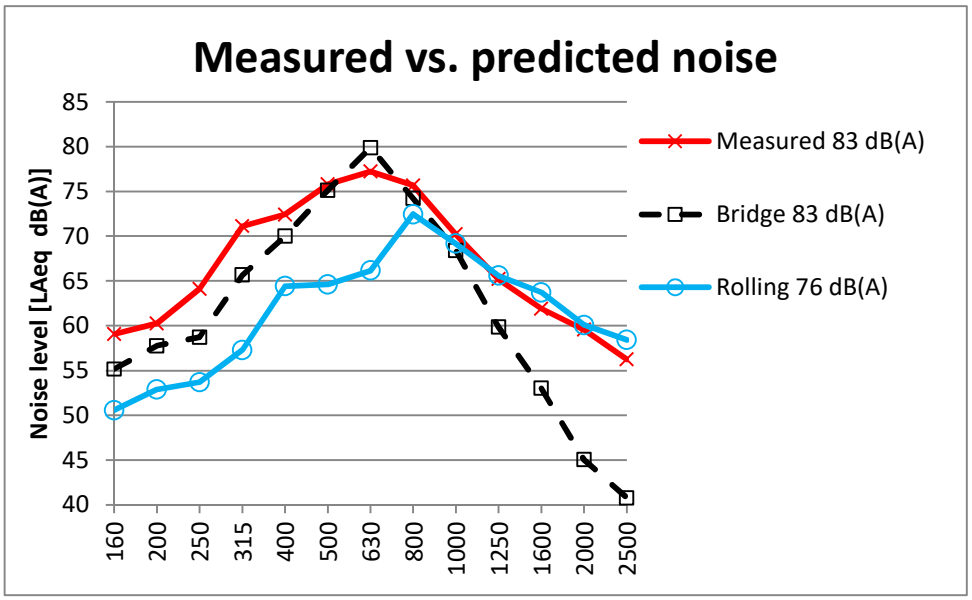

Figure 15 – A-weighted 1/3-octave band spectra at Pos A, measured and predicted spectra.

One step further, the prediction model shows the distribution and ranking of noise contributions from the different bridge components for the untreated bridge, see Figure . It follows that the most significant components are the deck, and longitudinal girders. From Figure it can be assessed that the potential for noise reduction based entirely on reducing the bridge contribution is approximately 7 dB, in the hypothetical case that the bridge radiated noise is reduced by about 20 dB or more.

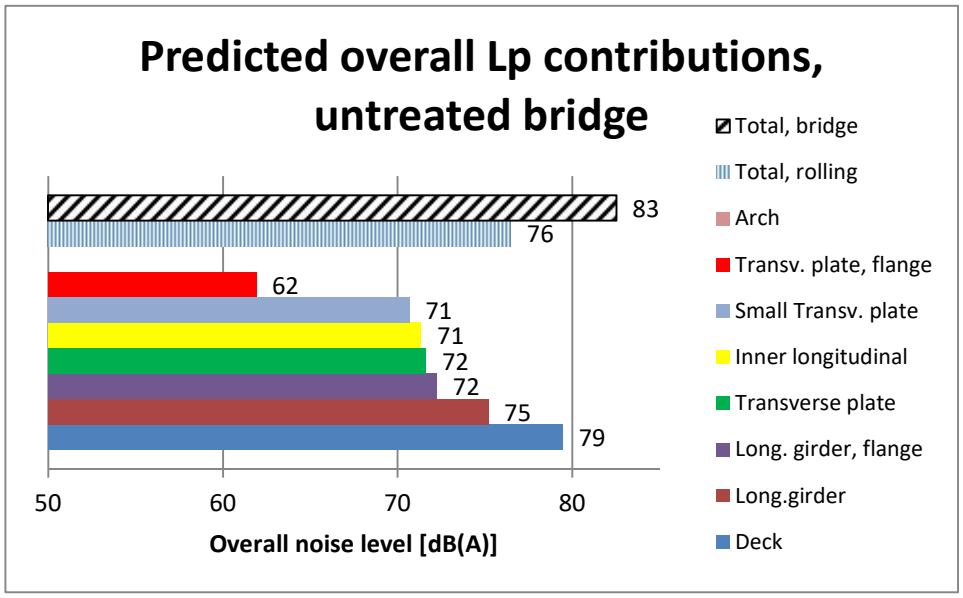

Figure 16 – Distribution of component related noise contributions for untreated bridge.

With reference to the prediction results of the untreated bridge, the noise at Pos A for each of the CLD configurations was calculated using the prediction model. It was found that the bridge noise contribution could be reduced by up to 8 dB. The overall noise, when including train/rolling noise, could be reduced by up to 4 dB by several the CLD configurations. As illustration, the predicted, detailed reduction corresponding to the use of Sample ID 3(Shaker ref. A) is shown in Figure 17.

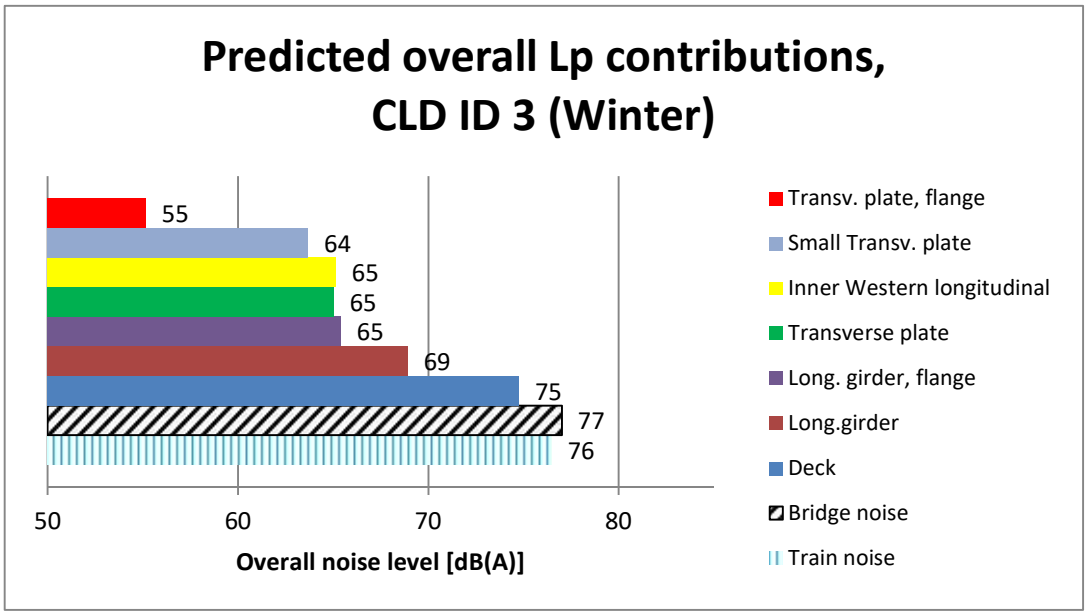

Figure 17 – Example of predicted noise reduction for winter temperature using CLD ID 3(shaker ref. A). Predicted overall level is 80 dB(A), corresponding to a reduction of 4 dB. Reduction of the bridge noise is 6 dB.

4. Final remarks

Using a combination of different measurement techniques and numerical modelling, a simple prediction model was established for the train passage noise. Introduction of laboratory based damping data for various Constrained Layer Damping (CLD) solutions, allowed assessment of the potential for noise reduction by means of only treating the bridge components. A significant potential was found. Furthermore, it was found that CLDs based on specific combinations of two viscoelastic materials could provide relatively consistent noise reduction across frequency and temperature.

Based on the presented findings, the Swedish Transport Administration is currently considering which noise control strategy to implement for the Old Årsta bridge.

ACKNOWLEDGEMENTS

This study was financed by the Swedish Transport Administration and SKANSKA, and the authors wish to express their gratitude to these organisations for constructive collaboration. In addition, thanks to the many colleagues at Vibratec and LR who helped with the project.

REFERENCES

1. Thompson D. Railway Noise and Vibration. Oxford, UK: Elsevier; 2009.
2. Cox S. Railway noise: some case studies of different problems with different solutions. In: Proc AusRAIL PLUS 2007; 4-6 December 2007; Sydney, Australia 2007.
3. Olsen A. Lützen RS. Vibration Damping of air intake filter for gas engine, using constrained layer damping (CLD). In: Proceedings of Baltic-Nordic Acoustic Meeting (BNAM); 2016 June 20-22; Stockholm, Sweden 2016
4. Railway steel bridges [Internet]. 2017 [cited 2017 May 5]. Available from http://www.sundv.de/en/steel-bridges.html
5. Jones David I.G. Handbook of viscoelastic vibration damping. Chichester, UK: Wiley & sons; 2001
6. Nashif A. Jones D I.G. Hendenson J. Vibration damping. Dayton Ohio; Wiley & sons; 1984